BeFo

STIFTELSEN BERGTEKNISK FORSKNING
ROCK ENGINEERING RESEARCH FOUNDATION

LABORATORY SIMULATION OF BLASTING INDUCED BOND FAILURE BETWEEN ROCK AND SHOTCRETE

Lamis Ahmed

BeFo Report 116

Cover figure:
Bond failure between test beam and shotcrete overlay (Cement mortar)

Omslagsbild:
Vidhäftningsbrott mellan provbalk och pågjuten sprutbetong (cementbruk)

STIFTELSEN BERGTEKNISK FORSKNING
ROCK ENGINEERING RESEARCH FOUNDATION

LABORATORY SIMULATION OF BLASTING INDUCED BOND FAILURE BETWEEN ROCK AND SHOTCRETE

Laborativ simulering av spränginducerat vidhäftningsbrott mellan berg och sprutbetong

Lamis Ahmed, KTH

BeFo Report 116
Stockholm 2012
ISSN 1104 – 1773
ISRN BEFO-R—116—SE

Preface

Rock support is an element of vital importance to ensure safety of the underground space we build. Shotcrete is today used as support in almost all underground structures, and the support strength depends of material properties, rock surface conditions, how the shotcrete is applied, and of vibration from blasting ort other. It is known that fresh concrete is affected by vibrations and it is important to clarify these effects on shotcrete in conjunction with blasting. The issue of curing time and distance to blasts is central in order to judge when and where next blast round can be performed. Excess margins due to uncertainty of how shotcrete is affected tend to result in more expensive facilities and longer construction time. Possible damage of the shotcrete support may affect the safety.

To improve the understanding of how vibrations affect young and hardened shotcrete, laboratory analyses and numerical finite element analyses were carried out. The resulting laboratory work was then used as input to a numerical model for calibration purpose. Thereafter, the numerical model was used to calculate load cases with different distances to the source of vibration and varying curing time for the shotcrete. These were then compared to actual cases from projects built. The laboratory tests were performed at the KTH Betongbyggnad laboratory in model scale.

The research was performed by the doctorate student Ms Lamis Ahmed at the Royal Institute of Technology (KTH) in Stockholm, Sweden. The work was supervised by Professor Anders Ansell, and resulted in a licentiate exam. Since additional research is needed in order to understand these mechanisms, this is planned and should result in a PhD exam.

The Rock Engineering Research Foundation, BeFo, have together with Formas financed this work which was completed in 2012. The researcher was supported by an advisory group consisting of Mikael Hellsten from BeFo, Jonas Holmgren, Anders Bodare and Richard Malm from KTH.

Stockholm in December 2012

Per Tengborg

Förord

Förstärkning av tunnlar och andra undermarkskonstruktioner är avgörande för säkerheten i de utrymmen som byggs. Sprutbetong används idag som förstärkning i nästan alla undermarksprojekt och dess hållfasthet beror av de ingående materialen, bergytans beskaffenhet, hur sprutbetongen appliceras och av vibrationer från sprängning eller annat. Det är känt att färsk betong påverkas av vibrationer, och det är viktigt att klargöra effekter på sprutbetong i samband med sprängning. Frågan om härdningstid och vilket avstånd till sprängning som behövs är central för att kunna avgöra när och var nästa sprängsalva kan skjutas. Onödigt stora marginaler på grund av osäkerhet om hur sprutbetongen påverkas leder till dyrare anläggningar och längre byggtid. Eventuella skador på sprutbetongförstärkningen kan i förlängningen påverka säkerheten.

För att öka förståelsen om vibrationers påverkan på ung respektive hård sprutbetong har man i detta forskningsprojekt utfört laboratorieförsök och numeriska analyser. Genom att ta fram indata från laboratorieförsök till numeriska analyser kan man kalibrera sin numeriska modell och göra beräkningar för olika fall. Därefter har olika avstånd till vibrationskällan och varierande härdningstid för sprutbetongen beräknats i den numeriska modellen för att få fram underlag som kan jämföras med de praktiska mätningar som utförts i några projekt. Laboratorieförsöken genomfördes i KTH Betongbyggnads laboratorium i modellskala.

Forskningen har resulterat i en uppfattning om acceptabla vibrationsnivåer och har utförts vid KTH av doktorand Lamis Ahmed. Forskningsarbetet som leddes av Professor Anders Ansell resulterade i en licentiatexamen. Fortsatta arbeten inom området behövs för att bygga upp kunskapen inom området vilket också planeras som underlag till en doktorsavhandling.

Stiftelsen Bergteknisk Forskning, BeFo, har tillsammans med Formas finansierat forskningen som slutfördes under 2012. Till projektet har knutits en referensgrupp bestående av Mikael Hellsten från BeFo, Jonas Holmgren, Anders Bodare och Richard Malm från KTH.

Stockholm i december 2012

Per Tengborg

Acknowledge

The work presented in this report was carried out at the Royal Institute of Technology (KTH), Division of Concrete Structures. The study was made possible through financial support from BeFo (Rock Engineering Research Foundation), supporting the laboratory experiments included in the project *Observation and vibration measurements of shotcrete exposed to blasting* which is hereby gratefully acknowledged.

I would like to express my sincere thanks and gratitude to my supervisor Professor Anders Ansell and assistant supervisor Dr. Richard Malm for their guidance, assistance, supervision, and encouragement during the term of this project.

I also wish to express my grateful thanks to the staff of the laboratory; Stefan Trillkott and Claes Kullberg at Department of Civil and Architectural Engineering at KTH for providing all the necessities for executing the laboratory works.

Stockholm, October 2012

Lamis Ahmed

Summary

In underground construction and tunnelling, the strive for a more time-efficient construction process naturally focuses on the possibilities of reducing the times of waiting between stages of construction. The ability to project shotcrete (sprayed concrete) on a rock surface at an early stage after blasting is vital to the safety during construction and function of e.g. a tunnel. A complication arises when the need for further blasting affects the hardening of newly applied shotcrete. If concrete, cast or sprayed, is exposed to vibrations at an early age while still in the process of hardening, damage that threatens the function of the hard concrete may occur. There are still no established guidelines for practical use.

It is, however, concluded from previous investigations that shotcrete can withstand high particle velocity vibrations without being seriously damaged. Shotcrete without reinforcement can survive vibration levels as high as 0.5−1 m/s while sections with loss of bond and ejected rock will occur for vibration velocities higher than 1 m/s. The performance of young and hardened shotcrete exposed to high magnitudes of vibration is currently investigated to identify safe distances and shotcrete ages for underground and tunnelling construction, using numerical analyses and comparison with measurements and observations. The work focuses on finding correlations between numerical results, measurement results and observations obtained during tunnelling. The outcome will be guidelines for practical use.

Simulation of stress wave propagation through good quality granite, from an explosive charge towards a shotcreted rock surface, has been performed in the laboratory. A non-destructive laboratory experiment was set up with P-wave propagation along a concrete beam. Cement based mortar with properties that resembles shotcrete was applied on one end of the beam, with a hammer impacting the other. Due to practical reasons the rock was made of concrete with similar dynamic properties as rock. The shotcrete was here substituted with cement mortar cast onto one of the quadratic end-surfaces of the concrete beam. The mortar thus formed a slab with the same cross section as the beam, bonding to the end-surface of the beam that corresponds to the rock surface in a tunnel.

The shape of the stress waves travelling towards the shotcrete was registered using accelerometers positioned along the bar. Finite element modelling was used to verify

the test results, which showed that the laboratory model with an impacting hammer could be used to initiate the same type of stress waves that is the result from blasting in good quality rock. Previously recommended maximum allowed peak particle vibration velocities were thus experimentally verified.

Sammanfattning

Inom tunnel- och undermarksbyggande innebär strävan efter en mer miljövänlig och tidseffektiv byggprocess att väntetiderna mellan byggetapper måste reduceras. Funktionen och säkerheten hos t.ex. en tunnel upprätthålls bl.a. av sprutbetong som anbringas på bergytorna omedelbart efter sprängning. Vid byggande i berg är begränsad kunskap om sprutbetongs motståndskraft mot vibrationer till stor nackdel, särskilt för entreprenörer vilka måste kunna planera och samordna resurser och olika insatser. Till exempel vid drivning av tunnlar vill man veta hur nära sprutbetong sprängning kan ske och dessutom hur lång härdningstid som krävs innan sprutbetongen uppnått tillräcklig hållfasthet. De väntetider och överdimensioneringar som idag måste accepteras motsvarar stora merkostnader vilket försvårar ett säkert och kostnadseffektivt bergbyggande. Det är också osäkert hur eventuella skador på sprutbetong som uppstår under byggskedet kommer att påverka tunnlarnas framtida funktion.

I de flesta underjordsarbeten i hårt berg används sprängämnen för att möjliggöra borttransport av bergmassor. Detta ger upphov till vibrationer i berget vilka fortplantas som spänningsvågor fram emot eventuella frilagda bergytor som förstärkts med sprutbetong. Höga spänningsnivåer kan leda till bortfall av vidhäftning mellan berg och sprutbetong eller utstötning av hela sprutbetongpartier. Problem kan t.ex. uppstå när parallella tunnlar drivs nära varandra eller när sprutbetong används nära tunnelfronten.

Slutsatsen från tidigare undersökningar visar att sprutbetong kan tåla höga vibrationer (partikelhastigheter) utan att allvarliga skador uppstår. Oarmerad sprutbetong kan vara oskadd efter att ha utsatts för så höga vibrationsnivåer som 0,5–1 m/s medan partier med förlorad vidhäftning till berget kan uppträda vid vibrationshastigheter högre än 1 m/s. Ett pågående forskningsprojekt fokuserar på jämförelser mellan resultat från framarbetade numeriska beräkningsmodeller och kunskap och erfarenheter från byggverksamhet. Funktionen hos ung och hårdnande sprutbetong som utsätts för höga vibrationsnivåer undersöks för att identifiera säkra avstånd och sprutbetongåldrar för undermarks- och tunnelbyggande. Vid beräkningar med datormodeller varieras betongens åldersberoende egenskaper för att undersöka skadebenägenheten hos ung och nysprutad betong på olika avstånd från en detonerande laddning. Arbetet fokuserar på att finna samband mellan numeriska resultat, mätresultat och observationer från

tunnelbyggande. Resultaten utvärderas genom jämförelser med mätningar och observationer gjorda i fältmiljö varvid gynnsamma och ogynnsamma förhållanden kunnat identifieras. Det slutliga resultatet kommer att vara riktlinjer för praktisk användning.

Simulering av spänningsvågutbredning genom granit av god kvalitet, från en explosiv laddning mot sprutbetong på en bergyta, har utförts i laboratorium. Ett icke-förstörande försök utfördes med P-vågutbredning längs en betongbalk, med egenskaper som liknar berg. På grund av praktiska skäl ersattes berget av betong med liknande dynamiska egenskaper. Cementbaserat bruk med egenskaper som liknar sprutbetong applicerades på ena änden av balken vilket bildade en platta med samma tvärsnitt för att motsvara sprutbetong på bergytan i en tunnel. Spänningsvågor, liknande de som observerats i fält, inducerades vid den motsatta änden av balken med en stålhammare. Testerna simulerade inkommande spänningsvågor vilka ger upphov till tröghetkrafter som orsakas av accelerationerna som verkar på sprutbetongen. Dessa kommer i sin tur att reflekteras i gränssnittet mellan sprutbetong-berg (platta-balk), vilket kan orsaka bortfall av vidhäftning. Det är också möjligt att sprutbetong kan bortfalla på grund av låg draghållfasthet. Formen på de spänningsvågor som når sprutbetongen registrerades med accelerometrar placerade längs balken. Finita elementmodeller har använts för att verifiera testresultaten, som visade att experimentmodellen med en påverkande hammare kan användas för att initiera samma typ av spänningsvågor som från sprängning i berg av god kvalitet. Tidigare rekommenderade högsta tillåtna maximala partikelvibrationshastigheter verifierades.

Contents

Preface ..... **i**

Förord ..... **iii**

Acknowledge ..... **v**

Summary ..... **vii**

Sammanfattning ..... **ix**

1. Introduction **1**

1.1 Background 1

1.2 Analytical method 2

1.3 Vibration velocity 3

1.4 Bond strength 4

2. Stress waves in elastic materials **9**

2.1 Physical appearance of stress waves 9

2.2 Principal frequency 12

3. Experimental program **13**

3.1 Material properties of test-beam 13

3.2 Fabrication and curing 13

3.3 Mortar property 15

4. Laboratory investigation **19**

4.1 Preliminary test measurements and instrumentation 19

4.1.1 Force spectrum characteristics 21

4.1.2 Processing of transducer signals 22
4.2 Test set-up 26
4.3 Measurement results 27
4.4 Evaluation of results 30
4.5 Shotcrete bond stresses 33

5. Conclusions 37

5.1 Discussion 37
5.2 General conclusions 38
5.3 Further research 41

Bibliography 43

1. Introduction

1.1 Background

Over the last decades, shotcrete has become an important material for stabilising excavated tunnels and underground openings in hard rock. Shotcrete can be sprayed onto a horizontal or a vertical surface and is widely used for tunnelling works. Its unique flexibility in the choice of application thickness, material compositions (e.g. fibre content), output capacity and fast early strength development make shotcrete a material well suited for rock support. By the middle of the 20th century, the use of shotcrete as a support system became widespread, with an increasing need for reliable guidelines and calculation methods to control the mode of action of shotcrete in hard rock.

Detonation of explosives during excavations of tunnels and underground spaces give rise to stress waves that propagate through the rock and can, at high vibration levels, cause severe damage to such support systems. The wave propagation velocity is governed by the type of rock and is different for different types of waves, such as pressure waves (P-waves) and shear waves (S-waves). The P-wave propagates faster than the S-wave and is therefore the first to reach an observation point when both wave types have been generated simultaneously, e.g. from a blast round, see e.g. [16]. To allow efficient and safe tunnelling it is necessary to know when the bond between rock and newly sprayed shotcrete has reached a level where it can withstand vibrations and incoming stress waves.

To study the behaviour of shotcrete under dynamic loading, a non-destructive laboratory scale model was set up with P-wave propagation along a concrete bar, with properties similar to rock. Cement based mortar with properties that resemble those of shotcrete was applied on one end of the beam with a hammer impacting the other. The shape of the stress waves traveling towards the shotcrete was registered using accelerometers positioned along the beam, providing time series numerically integrated to particle velocities proportional to the stress in the material. The work was a part of a research project investigating analytical models for shotcrete exposed to blasting [5].

1.2 Analytical method

A reliable analysis method for practical use must be able to forecast the size and location of areas with damaged shotcrete in e.g. a tunnel, from the input of geometry and a prescribed amount of explosives. Damage on shotcrete on a rock wall from detonations inside the rock, perpendicular to the wall, must be predicted and also the damage along the tunnel walls from detonations at the tunnel front. The studied problem is complex and requires an extensive numerical modelling effort where the character of the loads from blasting are studied in detail followed by numerical simulations to describe wave propagation through the rock, towards the shotcrete. A research project reported in 2012 [5] involved development of sophisticated dynamic finite element models for which the collected information and data from the laboratory tests described in this report will be used as input. The models were evaluated and refined through comparisons between calculated and measured data. First were existing, simple prototype models compared and evaluated through calculations and comparisons with existing data [6]. The first model tested is a structural dynamic model that consists of masses and spring elements. The second is a model built up with finite beam elements interconnected with springs. The third is a one-dimensional elastic stress wave model. The stress response in the shotcrete closest to the rock when exposed to P-waves striking perpendicularly to the shotcrete-rock interface was simulated. Results from a non-destructive laboratory experiment were used to provide test data for the models [7]. Based on experience from the prototype models the finite element program Abaqus was then used for the development of more detailed models, based on solid finite elements [4]. Due to the inhomogeneous nature of the rock, the stress waves from the blasting attenuate on the way from the point of explosion towards the shotcrete on the rock surface. Material damping for the rock mass is therefore accounted for, estimated from previous in-situ measurements. The vibration resistance of the shotcrete-rock support system depends on the material properties of the shotcrete and age-dependent properties were varied to investigate the behaviour of young shotcrete subjected to blast loading. The numerical simulations require insertion of realistic material data for shotcrete and rock. To evaluate the propagation of the stress waves in rock and young and hardening shotcrete focus was put on the development by age of properties such as the elastic modulus and the bond strength between shotcrete and rock.

The calculated results were in good correspondence with observations and measurements in situ, and with the previous numerical modelling results. Compared to the prototype models, using a sophisticated finite element program to facilitate modelling of more complex geometries and also provide more detailed results. The models must include the properties of the rock and the accuracy of the material parameters used will greatly affect the results. However, this also means that it will be

possible to describe the propagation of the waves through the rock mass, from the centre of the explosion to the reflection at the shotcrete-rock interface. Using a sophisticated finite element program with elastic models in dynamic analyses gives a relatively efficient and fast analysis process. It is acceptable to use elastic material formulations until the material strengths are exceeded, i.e. until the strains are outside the elastic range which thus indicates a material failure. The higher complexity of this type of model, compared to the prototype models, will make it more demanding to validate the results since the relation between input-output is more complex. The advantage is that more sophisticated geometries can be modelled. Examples of preliminary recommendations for practical use are given and it is demonstrated how the developed models and suggested analytical technique can be used to obtain further detailed limit values. The project and connecting laboratory experiments are documented in three scientific papers [4, 6 and 7] and has also been presented at an international shotcrete conference [3] and at a symposium on Nordic concrete research [2]. The project is summarized in a licentiate thesis put forth in May 2012 [5].

1.3 Vibration velocity

Some previous attempts have been made to investigate the effect on shotcrete from blasting, with respect to the maximum vibration velocity that can be allowed. Maximum vibration levels are often defined in terms of peak particle velocity (PPV). In-situ tests, underground in the Swedish mine at Kiirunavaara [9, 10], were conducted with sections of plain, un-reinforced shotcrete projected on tunnel walls and exposed to vibrations from explosive charges detonated inside the rock. The response of the rock was measured with accelerometers mounted on the rock surface and 0.5 m into the rock. The observed vibration levels showed that sections of shotcrete had withstood high particle velocity vibrations without being seriously damaged. It was concluded that shotcrete without reinforcement, also as young as a couple of hours, can withstand vibration levels as high as 0.5−1.0 m/s, while section with loss of bond and ejected rock were found for vibration velocities higher than 1.0 m/s. Similar measurements, based on in-situ experiments conducted in Japan [29], showed that vibration velocities of 0.7 m/s cracked the observed shotcrete lining. The response of steel fibre-reinforced and steel mesh-reinforced shotcrete linings subjected to blasts was investigated in a Canadian mine [27, 39]. It was observed that the shotcrete remained attached to the rock surface for vibration levels up to 1.5–2 m/s, with only partial cracking observed in the shotcrete. During other in-situ investigations [21] it was observed that the damage that can be expected during tunnelling is radial cracking across the shotcreted face nearest the blast and transverse cracking, from the face and into the tunnel. Table 1.1 shows that the

bond between shotcrete and rock can withstand PPV levels in the range 0.5–2 m/s before damage occurs.

Table 1.1: Vibration velocities (PPV) when bond damage occurs. Based on in-situ measurements.
Vibrationshastigheter (PPV), då bortfall av vidhäftning mellan berg och sprutbetong sker. Från fältmättningar.

	PPV	Comments
Kiirunavaara, Sweden [9, 10]	0.5−1.0 m/s	Young shotcrete
Tunnelling, Japan [29]	up to 0.7 m/s	
Gold mine, Canada [27, 39].	1.5–2.0 m/s	Steel fibre-reinforced and steel mesh-reinforced shotcrete

1.4 Bond strength

Hahn and Holmgren [18] suggested that the bond strength for shotcrete on granite should be set to 0.5–1.0 MPa at 28 days. However, in cases where significant fractures or other planes of weakness exist parallel to the shotcrete-rock interface, it must always be assumed that the effective bond strength will be low [13]. Low bond strength will also occur for surfaces not initially cleaned, which means that the bond can be improved by first washing the rock surface using high pressure water. The tests were carried out in a laboratory environment with sprayed concrete older than 28 days on rock panels with different surface configuration, smooth and rough. The type of rock mineral was found to be more important than the roughness of the surface and one important conclusion is that an increase in bond strength due to a rough surface is mainly caused by the surface magnification gained compared to a smooth surface, see Figure 1.1 The influence of surface roughness has also been studied by Kumar *et al*. [23] who present test results within 0.1–0.5 MPa for sandstone and shale. They also conclude that there is no effect on the bond strength from an increase in tensile strength of the rock. The importance of a clean rock surface was pointed out already by Barbo [12], who showed that surfaces polluted by diesel exhausts reduces the bond strength, and by Karlsson [20] who showed that free water on the rock surface has a negative effect. Saiang *et al.* [33] performed a series of laboratory tests on cemented shotcrete-rock joints, to investigate the strength and stiffness of the interfaces. The load at which two jointed pieces came apart was considered as the bond strength. Average bond strength of 0.56 MPa was obtained. Malmgren *et al.* [25] investigated the influence of surface treatment of rock (water jet scaling), shrinkage and hardening of shotcrete on the bond strength. The bond tests were carried out in accordance with the Swedish standard [35]. Three different

methods of rock surface preparation were tested; mechanical scaling, scaling and high-pressure water washing and water-jet scaling. The results show that over a third of the tests done on areas with only mechanical scaling showed no bond between rock and shotcrete. For the other two categories only 7–17 % of the tests resulted in zero bond strength which demonstrate the importance of spraying on a well-cleaned rock surface. The results also showed overall poor bond strength of 0.3–0.4 MPa between shotcrete and the iron ore in the mine where the tests were conducted. Other, small scale tests carried out in the same mine shows values as high as 0.7–1.1 MPa [10]. Another interesting test was done in a Canadian mine where the rock type was quartz diorite of good quality [31]. It was evident, also in this case, that the measured strength values depend on roughness and shape of the rock surface. It is of interest to compare these results with the bond possible to obtain between shotcrete and cast concrete. Tests with spraying on a well-cleaned concrete wall were done by Malmgren *et al.* [25] presenting values within 0.6–2.0 MPa. It should be noted that the concrete surface had been sandblasted prior to spraying. The bond strength between old concrete, worked by jackhammer, and shotcrete is presented by Silfwerbrand [34]. The results from the pull-out tests show values between 1–2 MPa. It is interesting to note that torsional testing in the same material gave higher values for the bond shear strength, i.e. in the direction parallel with the interface between the sprayed and cast material. The examples discussed above are summarized in Table 1.2. For comparison are also values obtained during tunnelling work given, [17 and 24]. Furthermore, a series of tests with a new approach for testing the bond strength between young shotcrete and a concrete plate, was performed by Bryne *et al.* [15]. The tests indicated a relatively rapid development of the bond strength which reached 1.0 MPa after 24 hours. This is in good correspondence to the range of 0.6–1.1 MPa reported from other investigations on 1–2 days old shotcrete and mortar [15]. The above bond strength values obtained for young and hardened shotcrete are summarized in Table 1.3.

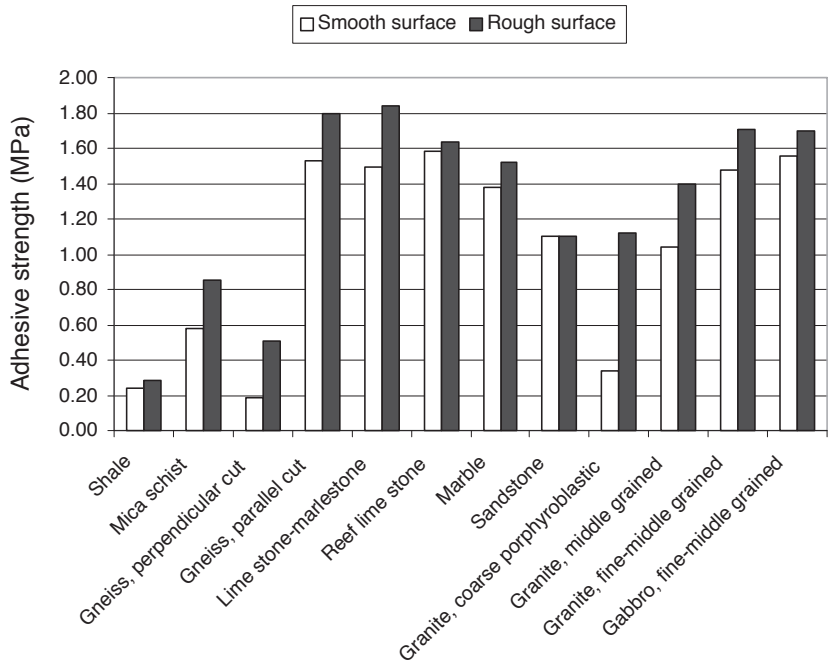

Figure 1.1: Expected bond strength between shotcrete and various types of rock, according to Hahn and Holmgren [18]. Figure from [11].
Förväntad vidhäftning mellan sprutbetong och olika typer av berg, enligt Hahn and Holmgren [18]. Figur från [11].

Table 1.2: Examples of bond strength obtained for fully hardened shotcrete, sprayed on different surfaces. Results from pull-out tests [15].
Exempel på vidhäftningshållfasthet hos hårdnade sprutbetong applicerad på olika ytor. Resultat från vidhäftningsprov [15].

Bond strength (MPa)	**Surface**	**Reference**
0.1–0.3	Shale	Kumar et al. [23]
0.2–0.3	Shale	Hahn and Holmgren [18]
0.6–0.9	Mica schist	Hahn and Holmgren [18]
0.1–0.5	Sandstone	Kumar et al. [23]
1.1	Sandstone	Hahn and Holmgren [18]
0.3–0.4	Magnetite (iron ore)	Malmgren *et al*. [25]
0.7–1.1	Magnetite (iron ore)	Ansell [10]
1.4–1.5	Marble	Hahn and Holmgren [18]
0.3–1.7	Granite	Hahn and Holmgren [18]
1.6–1.7	Gabbro	Hahn and Holmgren [18]
0.2–1.8	Gneiss	Hahn and Holmgren [18]
1.5–1.8	Lime stone	Hahn and Holmgren [18]
1.0–3.0	Quartz diorite	O'Donnell and Tannant [31]
0.6–2.0	Concrete	Malmgren *et al.* [25]
1.0–2.0	Concrete	Silfwerbrand [34]
0.0–2.0	Usual results	Holmgren [19]
>0.5	At normal tunnelling conditions	Holmgren [19]
≤0.5	Recommendation, hard granite	Vandewalle [38]
1.4 (mean)	Tunnelling, wet-mix method	Ellison [17]
1.0 (mean)	Tunnelling, dry-mix method	Malmberg [24]
0.9 (mean)	Tunnelling, wet-mix method	Malmberg [24]

Table 1.3: Estimated bond strength at shotcrete-rock interface. From tests with cement mortar on concrete [15].
Beräknad vidhäftningshållfasthet i gränssnittet mellan sprutbetong-berg. Från prov med cementbaserat bruk på betong [15].

Age	Bond strength
6 hours	0.06 – 0.07 MPa
10 hours	0.36 MPa
12 hours	0.35 – 0.48 MPa
18 hours	0.67 – 0.83 MPa
24 hours	0.74 – 1.15 MPa

2.Stress waves in elastic materials

The main difference in a structural dynamic analysis, compared to a static analysis, is the inclusion of inertia effects caused by motion of masses. In this chapter, the stress wave propagation in elastic media is described and the elastic stress wave theory reviewed. As a complement, a brief derivation of the natural frequencies for a longitudinally vibrating bar, or beam, is given.

2.1 Physical appearance of stress waves

An elastic body with large extensions in all three dimensions can be approximated by a smaller volume restricted by boundaries given physically relevant properties, i.e. boundary conditions. This approximation is accurate if the length of waves travelling in the body is small compared to its dimensions [9]. In light of this assumption, the stress wave propagation may be treated by means of a one-dimensional approximation. The following section briefly describes the approach to understand the underlying theory of one-dimensional wave propagation in elastic solids, which is based on [28]. To derive the equation of motion for longitudinal vibration, the axial deformation of a long, thin member can be considered, as shown in Figure 2.1(a). A freebody diagram for an element of length *dx* is shown in Figure 2.1(b).

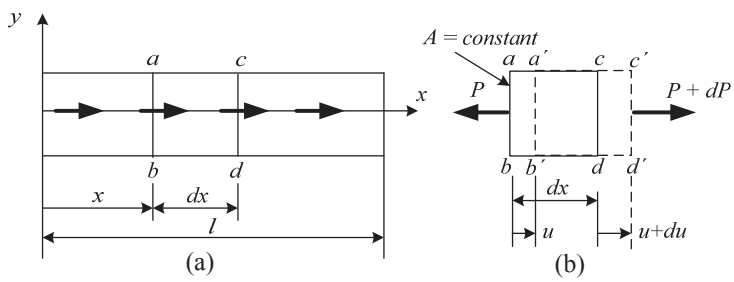

Figure 2.1: Member undergoing axial deformation (a) and free body diagram (b).
Element under axiell deformation (a) och friläggningsdiagram (b).

The force acting on the cross section of a small element of the bar is given by P and P+dP with

$$P = \sigma A = A E \frac{\partial u}{\partial x} \tag{2.1}$$

where $\partial u / \partial x$ is the axial strain, obtained by applying Newton's second law

$$\sum F_x = (\Delta m)\ddot{u} \tag{2.2}$$

The summation of the forces in the x-direction gives the equation of motion (as shown in Figure 2.1) where $f(x,t)$ denotes the external force per unit length,

$$(P + dP) + f\,dx - P = \rho \mathrm{A}\,\Delta x \ddot{u} \tag{2.3}$$

where ρ is the density of the media. By using the relation $dP = (\partial P / \partial x)\,dx$ and Eq. (2.1), the equation of motion for the forced longitudinal vibration of a uniform bar, can be expressed as

$$E\,A \frac{\partial^2 u}{\partial x^2}(x,t) + f(x,t) = \rho\, A \frac{\partial^2 u}{\partial t^2}(x,t) \tag{2.4}$$

where $\ddot{u} = (\partial^2 u / \partial t^2)$. This is the equation of motion for axial vibration of a linearly elastic bar. For the bar, the free vibration equation can be obtained from Eq. (2.4) by setting $f = 0$, as

$$c^2 \frac{\partial^2 u}{\partial x^2}(x,t) = \frac{\partial^2 u}{\partial t^2}(x,t) \tag{2.5}$$

where c is the propagation velocity. In a one-dimensional elastic body, e.g. a bar, the propagation velocities of longitudinal P-waves (c_p) and transverse S-waves (c_s) depends only on ρ and elastic constants, and are:

$$c_\mathrm{p} = \sqrt{\frac{E}{\rho}} \tag{2.6}$$

and

$$c_s = \sqrt{\frac{E}{\rho}\ \frac{1}{2(1+\upsilon)}} \tag{2.7}$$

where E is the elastic modulus of the material and υ the Poisson's ratio. When P-wave propagation is considered, which is the case for many construction and blast vibration problems [16], Eq. (2.5) should be employed.

The solution of Eq. (2.5), the wave equation, can be written as

$$u(x,t) = U(x)T(t) = (C_1 \cos\frac{\omega x}{c} + C_2 \sin\frac{\omega x}{c})(C_3 \cos\omega t + C_4 \sin\omega t) \tag{2.8}$$

where the function $U(x)$ represents the normal mode, depending on position along the x-axis, and the function $T(t)$, that depends on time t. To derive the stress wave propagation, $f = 0$ and $\partial P = \Delta\sigma$ A is inserted in Eq. (2.3), giving:

$$\Delta\sigma\ \mathrm{A} = (\rho\ \mathrm{A}\ \Delta x)\frac{\Delta v}{\Delta t} \tag{2.9}$$

where σ is the stress and v is the particle velocity. For the constant cross section area, Eq. (2.9) can be written as:

$$\Delta\sigma = \rho\,\frac{\Delta x}{\Delta t}\,\Delta v \tag{2.10}$$

where $\Delta x/\Delta t$ is equal to c. Then, Eq. (2.9) becomes:

$$\Delta\sigma = \rho\ c\ \Delta v \tag{2.11}$$

Generalizing the above equation, the time-dependent relation between the stress (σ) and the two velocities, particle velocity (v) and propagation velocity (c), is

$$\sigma(t) = \rho\ c\ v(t) \tag{2.12}$$

2.2 Principal frequency

To derive the natural frequencies for a longitudinally vibrating bar, the boundary conditions for the bar must be known. In this study, the case of free-free beam will be used together with the frequency equations for longitudinal vibration of uniform bars.

The frequencies are derived with Euler-Bernoulli beam theory; see e.g. [22, 37].

The boundary conditions of a free-free bar of length ℓ the boundary conditions are

$$\frac{\partial u}{\partial x}(0,t)=0 \tag{2.13}$$

and

$$\frac{\partial u}{\partial x}(\mathrm{l},t)=0 \tag{2.14}$$

Insertion of Eq. (2.13) in Eq. (2.8) gives C_1=0, while Eq. (2.14) gives the circular frequency equation

$$\sin\frac{\omega \mathrm{l}}{c}=0 \tag{2.15}$$

The eigenvalues or circular natural frequencies are given by

$$\omega_n=\frac{n c\,\pi}{l},\quad n=0,1,2,..... \tag{2.16}$$

These natural frequencies include a zero-frequency for n = 0, i.e. a rigid-body mode. The behaviour of such bars has been investigated experimentally, see Chapter 4. For n = 1 , the natural frequency is given by

$$f_1=\frac{\omega_1}{2\pi}=\frac{c\,\pi}{1}\cdot\frac{1}{2\pi}=\frac{c}{2\mathrm{l}} \tag{2.17}$$

3. Experimental program

A non-destructive laboratory experiment that studied wave propagation along a concrete beam, with properties similar to rock, was performed. Cement based mortar with properties that resembles shotcrete was applied on one end of the beam with a hammer impacting the other. In this chapter the properties of the concrete beam and cement based mortar are presented.

3.1 Material properties of test-beam

The test-beam was cast from concrete with a density ρ and a compressive strength f_{cc} of 2337 kg/m^3 and 81 MPa, respectively. The density is close to that of typical Swedish rock (granite), i.e. ρ = 2400–2700 kg/m^3 [9]. The average of the compressive strength (f_{cc}) for three control specimens 150 mm cube is shown in Table 3.1.

Table 3.1: The average of the density and compressive strength for control specimens.
Genomsnittlig densitet och tryckhållfasthet för kontrollprover.

Cube No.	Age at test (day)	Density (kg/m^3)	f_{cc} (MPa)
AA4	28	2341.0	76.0
AA5	28	2336.0	74.4
AA6	28	2333.0	74.7
Average		2336.6	75.0

3.2 Fabrication and curing

Two beams were cast in a mould, shown in Figure 3.1, consisting of 25 mm plywood. The dimensions of the beam were 0.3×0.3×2.5 m^3. Each beam was cast with three control 150 mm cubes. An electrical hand held vibrator was used to vibrate the concrete in the mould while a table vibrator was used to vibrate the control cubes. Finally, the top surface of the beams and the control cubes was smoothed. Curing consisted of keeping the beams and the control cubes at room temperature. Along the test-beam there were three different locations for fixing accelerometers, at the striking end, at mid-

length and at the far end. Slots were made with wood pieces mounted on the inner side of the mould, as shown in Figure 3.1b. Four accelerometers were mounted on the beam, three along the beam, as shown in Figure 3.2, and the forth one glued onto the end surface.

Figure 3.1: (a) Test-beam mould and (b) slot for accelerometers.
(a) Gjutform för balken och (b) plats för accelerometrar.

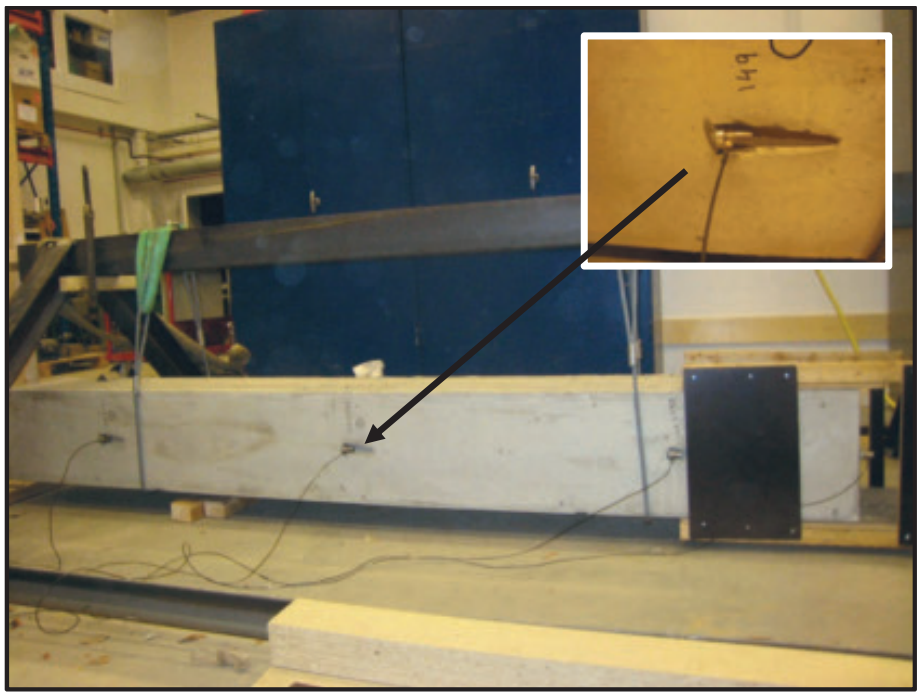

Figure 3.2: Accelerometers along the test-beam.
Accelerometrar längs balken.

3.3 Mortar property

The shotcrete was here substituted with cement mortar cast onto one of the quadratic end-surfaces of the concrete beam, as shown in Figure 3.3. The mortar thus formed a slab with the same cross section as the beam bonding to the end-surface of the beam that corresponds to the rock surface in a tunnel. The mortar used in place of shotcrete contained 1923 kg/m^3 aggregates within the fraction 0–6 mm, 427 kg/m^3 standard Portland cement and had a water-cement ratio of 0.45. A series of tests with 50 and 100 mm thick slabs of shotcrete (mortar) has been carried out where the beam with shotcrete was subjected to different intensity of impacts until failure. The tests were performed at shotcrete ages of 6 and 18 hours, as described in Table 3.2, which also give compressive strength from testing of 150 mm cubes.

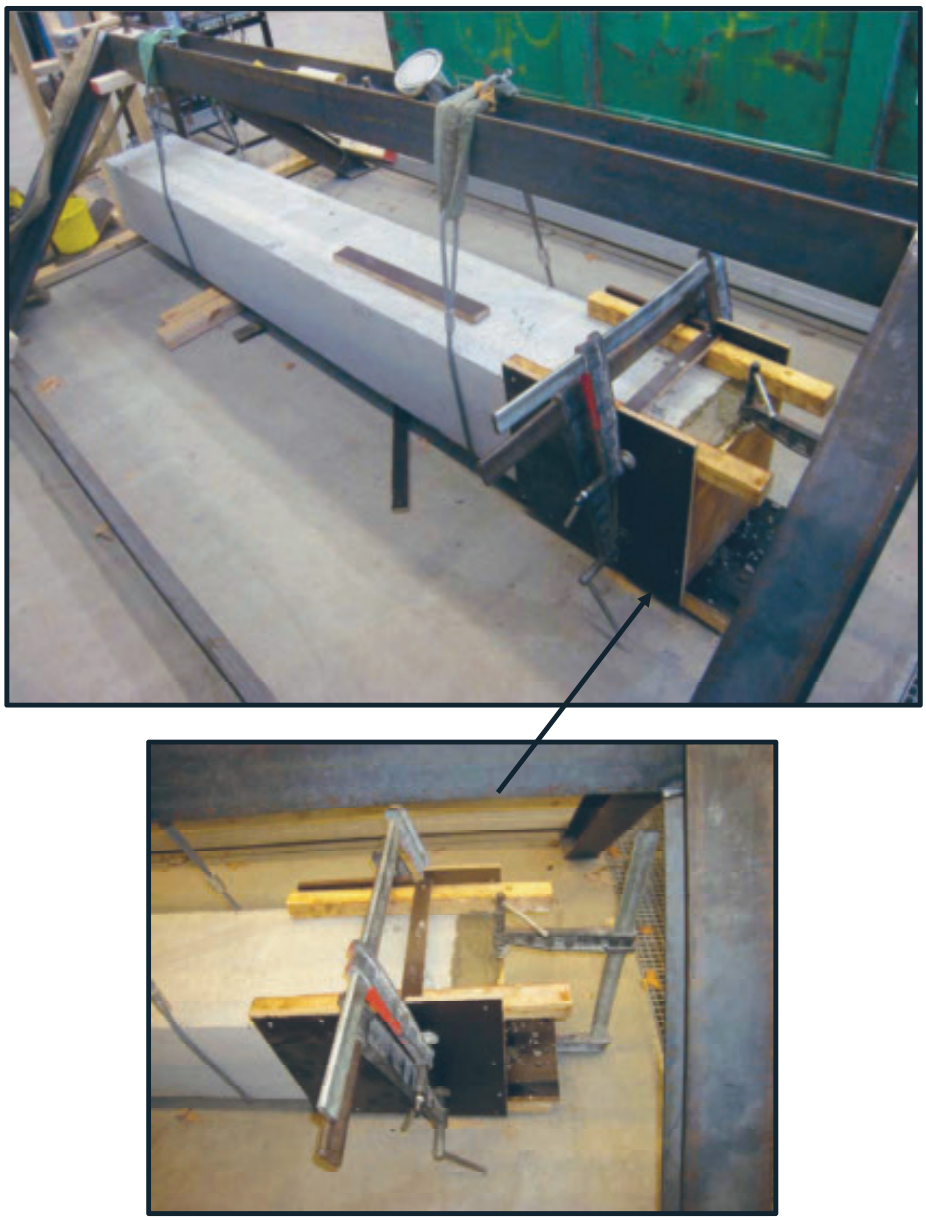

Figure 3.3: Casting of mortar.
Gjutning med murbruk.

Table 3.2: Test series.
Testserier.

Specimen type	Shotcrete thickness (mm)	Age (hrs.)	Density (kg/m^3)	Compressive strength (MPa)
BS50-6	50	6	2284	0.60
BS50-18	50	18	2242	17.0
BS100-6	100	6	2273	0.40
BS100-18	100	18	2268	21.6

4. Laboratory investigation

This chapter describes laboratory tests performed to simulate stress waves travelling through the rock, striking at the shotcrete and rock interface. The tests, also described in [7], give data to be used in the investigation and demonstration of how stress waves and structural vibrations are connected [5]. The results are also used for evaluation of the elastic stress wave model, see [7]. In addition, the bond strength development is investigated. It was concluded that the bond strength growth is initially faster than that of the compressive strength during the first 24 hours, see [7] for more details.

4.1 Preliminary test measurements and instrumentation

The impact device is a common excitation mechanism in modal testing. Although it is a relatively simple technique to implement, it is difficult to obtain consistent results. The method of applying the impulse is shown in Figure 4.1. The amplitude level of the energy applied to the structure is a function of the mass and velocity of the hammer. This is due the concept of linear momentum, which is defined as mass multiply by velocity.

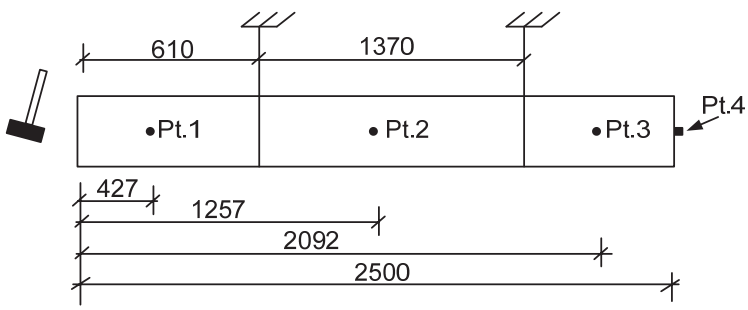

Figure 4.1: The location and numbering of the accelerometers.
Placering och numrering av accelerometrarna.

The impactor consists of a rigid mass (1720 g) with a force transducer attached to one end and an impact tip (139 g) attached to the opposite side of the force transducer, as shown in Figure 4.2. The test-beam was suspended with cables in a steel frame as shown in Figure 4.3. Four accelerometers were attached to the test-beams to measure the intensity and frequency spectrum of the shock vibration induced by the impactor blow. The forth one was glued onto the end surface, as shown in Figure 4.1.

Figure 4.2: Impactor.
Handhållen instrumenterad hammare.

Figure 4.3: Steel frame with suspended test-beam.
Stålram med hängande balk.

4.1.1 Force spectrum characteristics

In Figure 4.4, the frequency content versus the amplitude level of the energy applied to the beam can be seen. Since the force pulse usually is very short relative to the length of the time record, the portion of the signal after the pulse is noise, as shown in Figure 4.4 (a), and can be eliminated without affecting the pulse itself. The window designed to accomplish this, called a force window, is shown in Figure 4.4 (b).

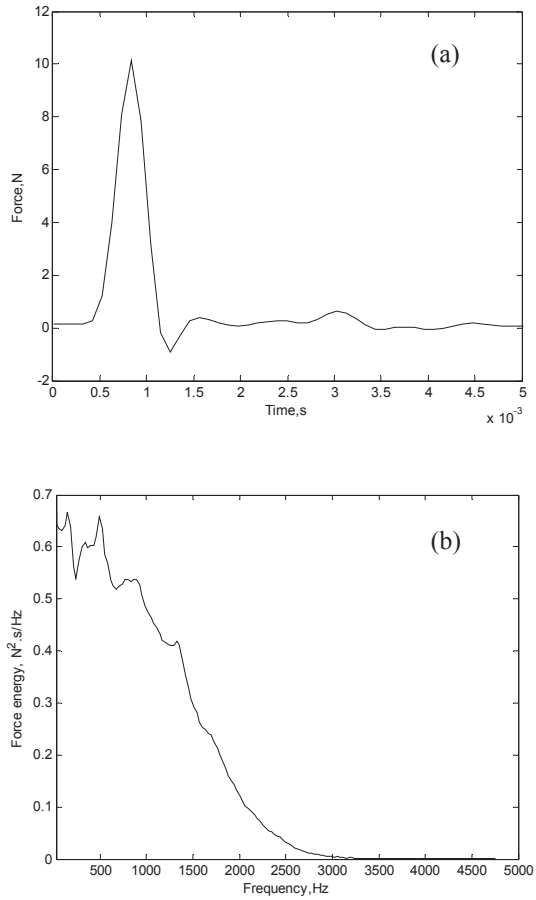

Figure 4.4: Typical force pulse and spectrum; (a) Impact force-time history, and (b) Impact force spectrum with rectangular window Aw=1.
Typisk impulskraft och spektrum; (a) impulskraft-tid, och (b) impulskraft spektrum med rektangulärt fönsterfunktion Aw=1.

4.1.2 Processing of transducer signals

Three accelerometers were positioned along the beam, with a fourth at the end surface, enabling recording of particle accelerations associated with stress waves traveling along the beam. The recording time was 0.1 s with a sampling frequency of 9600 Hz, the

highest possible. According to [36], the recorded signals of impact must be low-pass filtered before the data are sampled, as shown in Figure 4.5. To prevent out-of-band signals 'aliasing', the transducer signals were filtered using a low-pass (Bessel) filter within the data acquisition system. Frequency spectra were obtained using the fast Fourier transform (FFT) routines of the Matlab numeric software [26]. Using the FFT introduces limitations in the resolution of the spectrum so that it is only possible to obtain information on frequencies up to the Nyquist sampling frequency [36], i.e. here 4800 Hz.

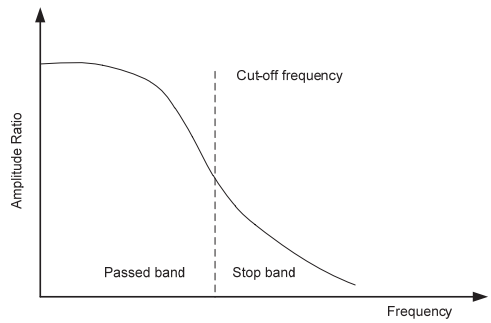

Figure 4.5: Low-pass filtering of frequency response.
Lågpassfiltrening av uppmätta frekvenssvar.

In Figure 4.6 – 4.9, the frequencies of the test-beam can be seen. The plot was produced using the algorithm [26] below:

```
n=6                          %n:th order of the filter
Fs=9600                      % Sampling frequency
f=3200                       % Cut off frequency
To create filtering the BUTTER and FILTER commends are used
[b,a]=butter(n,f/Fs,'low');
y=filter(b,a,x)  % x is a signal from the accelerometer
dt=1/Fs                      % time interval
N=length(y)                  % number of nodes
T=dt*N
f=0:1/T:Fs-1/T % frequencies along the x-axes in the spectrum
t=0:1/Fs:T-1/Fs
X=fft(y)                     % Fourier Transform
Aw=1                         % Rectangular windowing which used to reduce the
                             % leakage on the signal
Se=(Aw/N)^2
Lxx4=sqrt(Se*abs(X).^2)
```

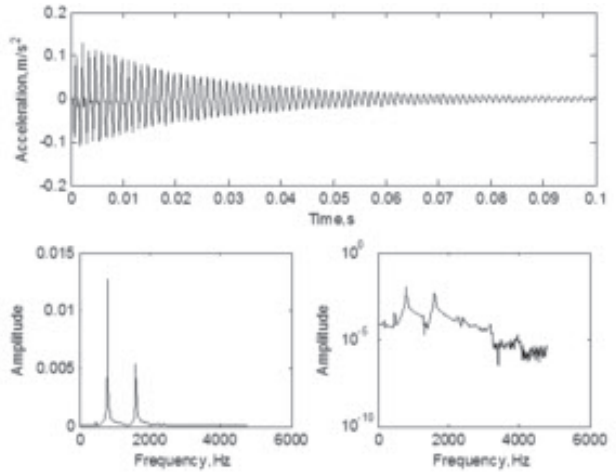

Figure 4.6: The acceleration-time history with filtering and the frequencies in normal and semilog y-scale for point 1.
Acceleration-tid med filtrering och frekvenserna i vanlig och semilog y-skala för punkt 1.

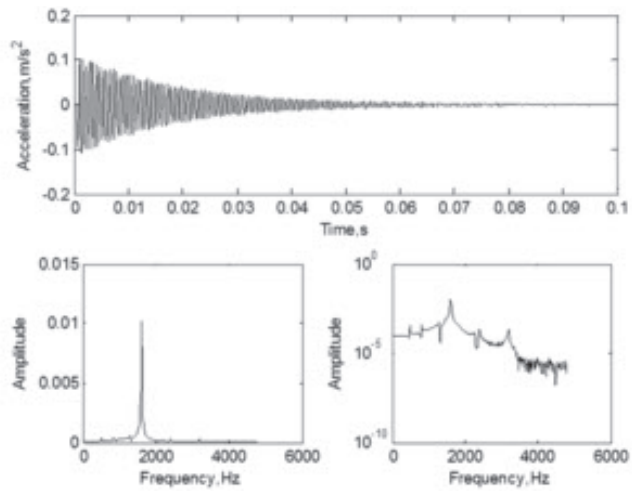

Figure 4.7: The acceleration-time history with filtering and the frequencies in normal and semilog y-scale for point 2.
Acceleration-tid med filtrering och frekvenserna i vanlig och semilog y-skala för punkt 2.

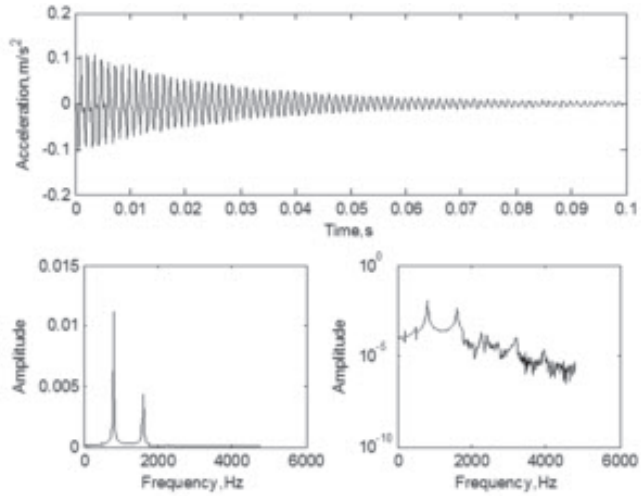

Figure 4.8: The acceleration-time history with filtering and the frequencies in normal and semilog y-scale for point 3.
Acceleration-tid med filtrering och frekvenserna i vanlig och semilog y-skala för punkt 3.

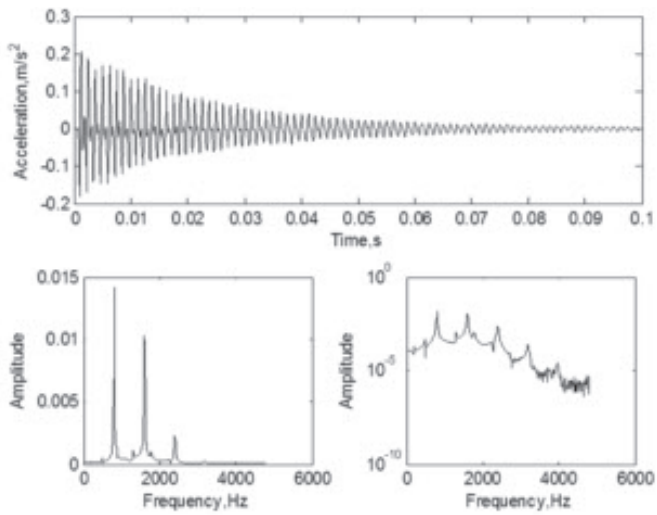

Figure 4.9: The acceleration-time history with filtering and the frequencies in normal and semilog y-scale for point 4.
Acceleration-tid med filtrering och frekvenserna i vanlig och semilog y-skala för punkt 4.

4.2 Test set-up

The set up for the used hammer impact test method is shown in Figure 4.10, with the concrete beam suspended in cables attached to a steel frame, as shown in Figure 4.11. The impacting hammer had a weight of 38.6 kg, a length (L_{imp}) of 0.3 m and a quadratic cross-section of 0.1×0.1 m^2. It was mounted on a swing arm, able to hit the beam end perpendicularly, as in Figure 4.10. When a stress pulse propagates along a rod, a bar or longitudinally along a beam, high frequency components propagate faster than low-frequency components resulting in dispersion of the pulse. This phenomenon is known as material dispersion, or attenuation in a two-dimensional case. Another type of dispersion, geometric dispersion, occurs when the wavelength of the stress wave is of the same order as the dimension of the cross section of the beam. Generally, to prevent the dispersion of the pulse, small dimensions are required so that the wavelength always is greater than the dimension of the beam [14]. The wavelength of the P-wave is twice the length of the impacting hammer [28]. Therefore, the wavelength of the P-wave transmitted in the test-beam is $2L_{imp}$ and equal to 0.6 m, a wavelength which is greater than the dimension of the beam (0.3 m). According to the pendulum equation applied for the hammer, the impact velocity is:

$$v_h = \sqrt{2gL(1-\cos\theta)} \tag{4.1}$$

where L is the length of the hammer arm, θ is the swing angle and g = 9.81 m/s^2 is the gravity constant.

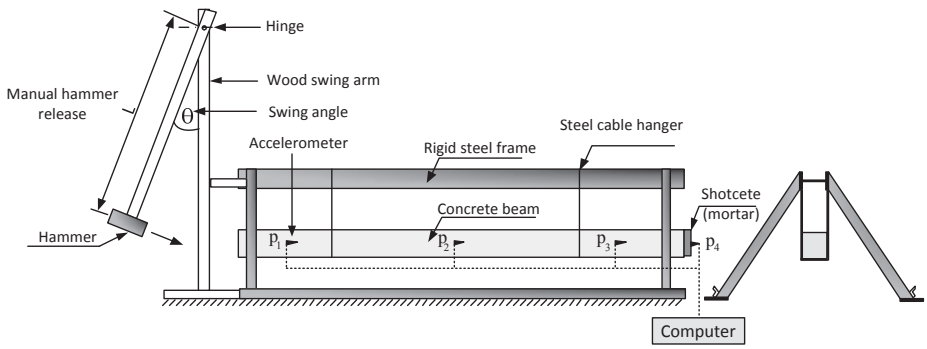

Figure 4.10: Schematic view of the set-up for hammer impact tests.
Schematisk bild av försöksuppställningen.

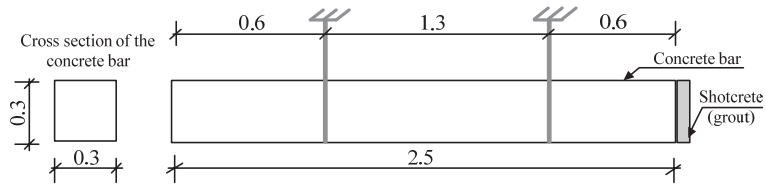

Figure 4.11: Details of the test-beam.
Försöksbalken.

In order not to exceed the accelerometer capacity, the length of the swing arm was here limited to 1.5 m and the tests carried out within swing angles of 5°–40°, corresponding to impact velocities between 0.33 and 2.6 m/s, including the range of interest, i.e. 0.5–1.5 m/s from the in situ observations.

Stress waves, similar to those observed in-situ, were induced at the opposite end of the beam through the impact of a steel hammer. The tests simulated incoming stress waves, giving rise to inertia forces caused by the accelerations acting on the shotcrete. These will in turn yield stresses at the shotcrete-rock (slab-beam) interface, which may cause bond failure. Note that in this case accelerometer point 4 is placed on the surface of the mortar, and not on the end of the concrete beam, as shown in Figure 4.1. It is also possible that shotcrete may fail due to low tensile strength, i.e. here a failure within the slab. The concrete beam with dimensions of $0.3\times0.3\times2.5$ m^3 is shown in Figure 4.11, with its material properties given in [7].

4.3 Measurement results

The measurements were divided into two parts; verification of the properties of the test-beam and the search for failure limit loads for the shotcrete. The first part was done to verify that the behaviour of the suspended test-beam is close to that of a free-free bar. Further details are presented in [7]. The acceleration-time history and acceleration–frequency spectra for the four points shown in Figure 4.10 of specimen BS100-18 are plotted in Figure 4.12. All acceleration-time histories and spectra that can be drawn from the performed measurements are similar to Figures 4.12. The results from the measured acceleration show that two waves propagate in opposite directions in the beam due to wave reflections; i.e. the incident wave and the reflected wave overlaps. Thus, the acceleration at the middle point (p_2) is the sum of the two opposing waves. When a propagating wave reaches the interface between shotcrete and rock, a part of the wave energy will be transmitted into the shotcrete while the other part reflects back into the rock.

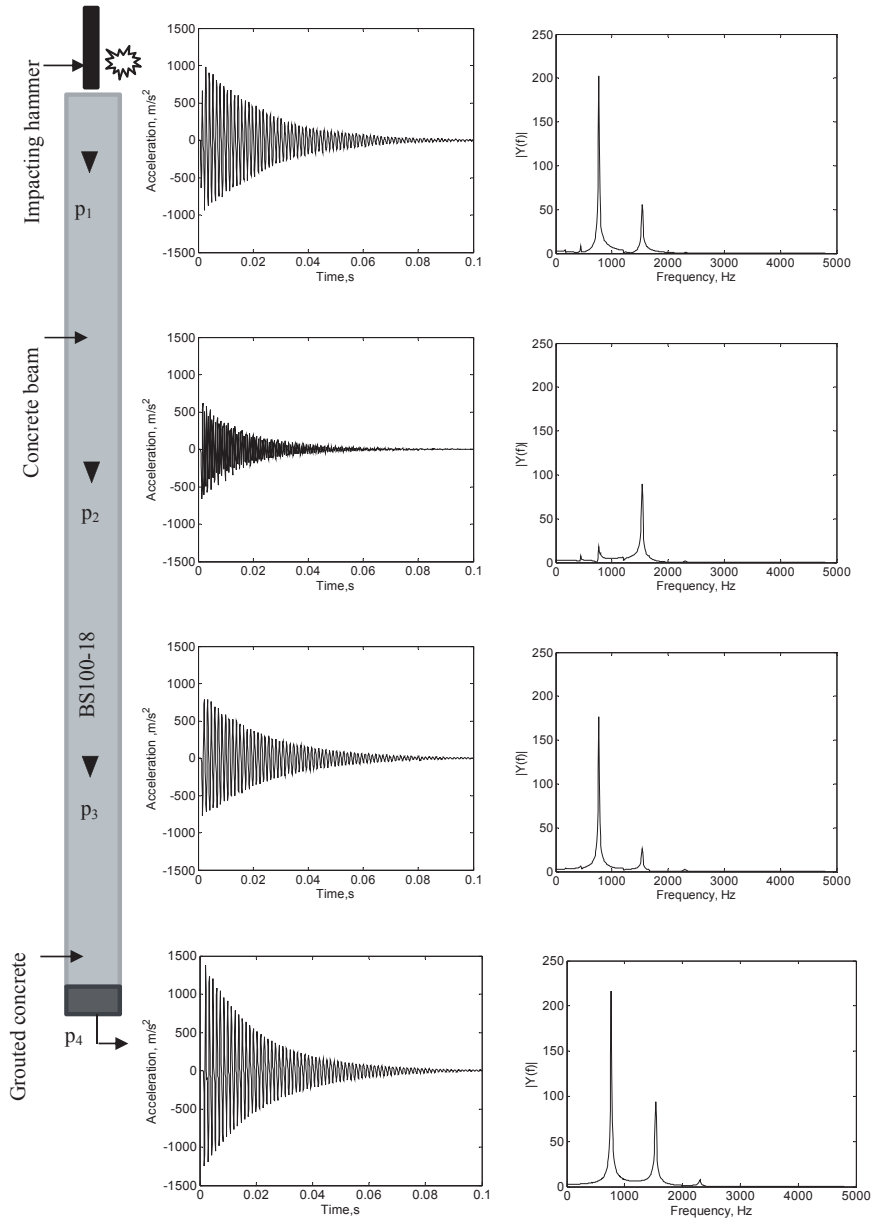

Figure 4.12: Measured acceleration-time history and frequency spectra, for an impact velocity of 1.85 m/s.
Uppmätt acceleration-tid och frekvensspektra för anslagshastigheten 1.85 m/s.

This proportion depends on the impedance ratio between rock and the shotcrete, see [7]. The transmitted wave propagates in the shotcrete and reaches the free surface where it is reflected back while doubling the acceleration; see e.g. Dowding [16].

The accelerometer measurements verified that the suspended test-beam has dynamic properties similar to a free-free bar. The results from the measurements of frequencies show that the longitudinal vibrations is dominated by the first vibration mode and that there is little contribution from the second mode, as shown in Figure 4.12. All results contain none or very small contributions from the third and higher modes and the used sampling frequency can therefore be accepted as accurate in this case. Figure 4.13 shows the acceleration on the shotcrete surface prior to failure and at failure, respectively. It can be seen from Figure 4.13 (a) that the shotcrete is rigidly tied to the concrete surface until failure occurs, as shown in Figure 4.13 (b), i.e. fully bonded until a sudden failure. Similar bond behaviour has been observed during testing [15]. By applying Eq. (2.17), it can be found that the concrete beam has a zero-frequency or rigid-body mode at $n = 0$. The modes corresponding to the non-zero frequencies of the concrete beam is shown in Figure 4.14.

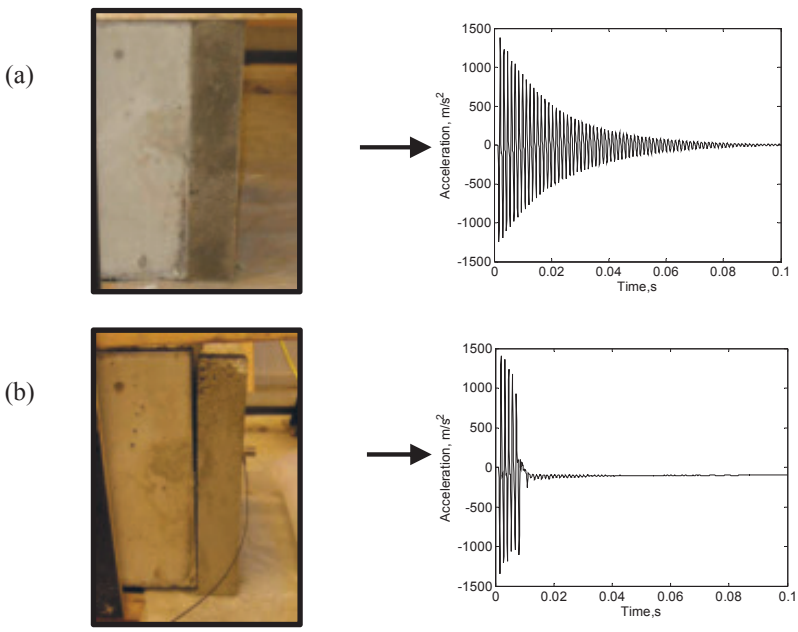

Figure 4.13: Frequency spectra from the measured accelerations, specimen BS100-18, (a) the impact velocity is 1.85 m/s and (b) the impact velocity is 1.92 m/s. *Frekvensspektra från uppmätta accelerationer, prov BS100-18; (a) med anslagshastighet 1.85 m/s och (b) med anslagshastighet 1.92 m/s.*

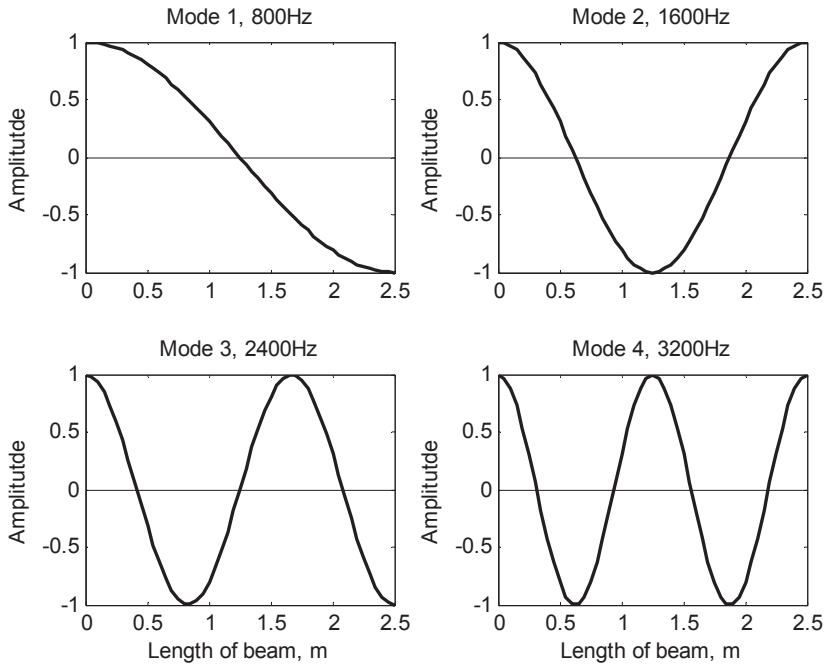

Figure 4.14: The longitudinal mode shapes of the free-free beam.
De längsgående modformerna för den fri-fria balken.

4.4 Evaluation of results

The engineering simulation program Abaqus [1] was used to create a three-dimensional FE model analyzed with the Abaqus/Explicit solver. A model of the test-beam is shown in Figure 4.15, the solid elements and features are presented in [7]. The interaction between the hammer, the concrete beam and the shotcrete layer were constrained using displacement boundary conditions, restricting the model to primarily describe particle displacements in the wave propagation direction. Between the concrete beam and the hammer free translation was only allowed in the longitudinal direction. The shotcrete was rigidly tied to the concrete surface to simulate the bond behaviour observed during testing [15]. The incident disturbing stress wave caused by the hammer was applied as surface to surface contact using the kinematic contact method with definition of the initial velocity in the longitudinal direction of the hammer, with the velocity assumed to follow Eq. (4.1). The acceleration-frequency spectra of the FE model were compared to the acceleration-spectra of the measured data to determine which element size and time

steps that could be used in the explicit analysis. The model consists of about 17000 nodes and 14000 elements.

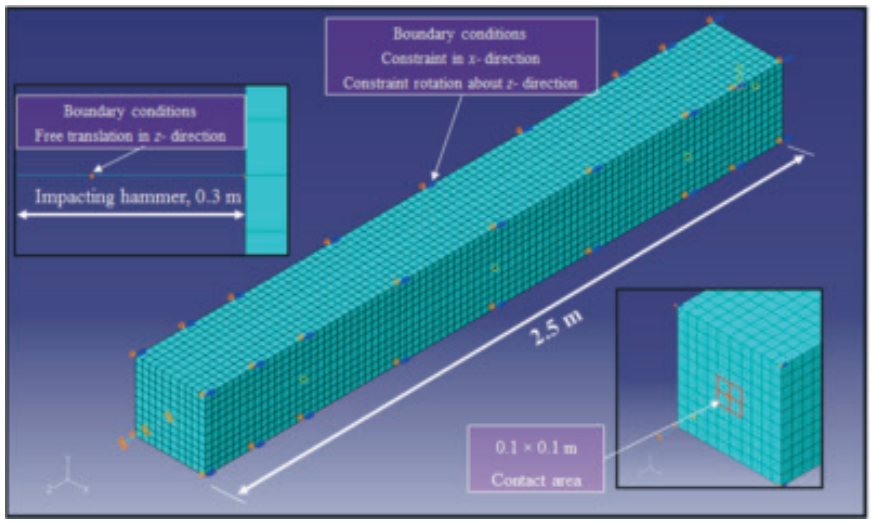

Figure 4.15: Finite element model of the experiment beam.
Finit elementmodell av den experimentella balken.

The acceleration-time history and acceleration-frequency spectra of simulated results for four points of specimen BS100-18 are plotted in Figures 4.16. The results from the FE models are in good agreement with the measured accelerations, shown in Figures 4.12 and 4.16. However, a fluctuation of the particle acceleration at the first measurement point (p_1) can be seen in the FE results. The impact produces compressive waves which propagate through the beam. At the same time release waves are generated at the free side surface and trail the main wave, as shown in Figure 4.17. These release waves interact continuously and cause fluctuation of particle acceleration and, consequently, of stress and strain at the surface of the beam [28]. The measured acceleration at p_1 demonstrate the same phenomenon, slightly different due to that the FE model provide more detailed results. The relation between impact velocities, according to Eq. (4.1), and integrated particle velocities from measured accelerations on the shotcrete surface is shown in Figure 4.18, together with the corresponding results from the FE model. Note that the straight lines representing the latter results diverge as the impact velocity increases, depending on age and thickness of the shotcrete. A good agreement between the simulated and measured results demonstrates that the kinematic contact method available in Abaqus can predict this type of impacts and that the results obtained using this model correlate well with the experimental results.

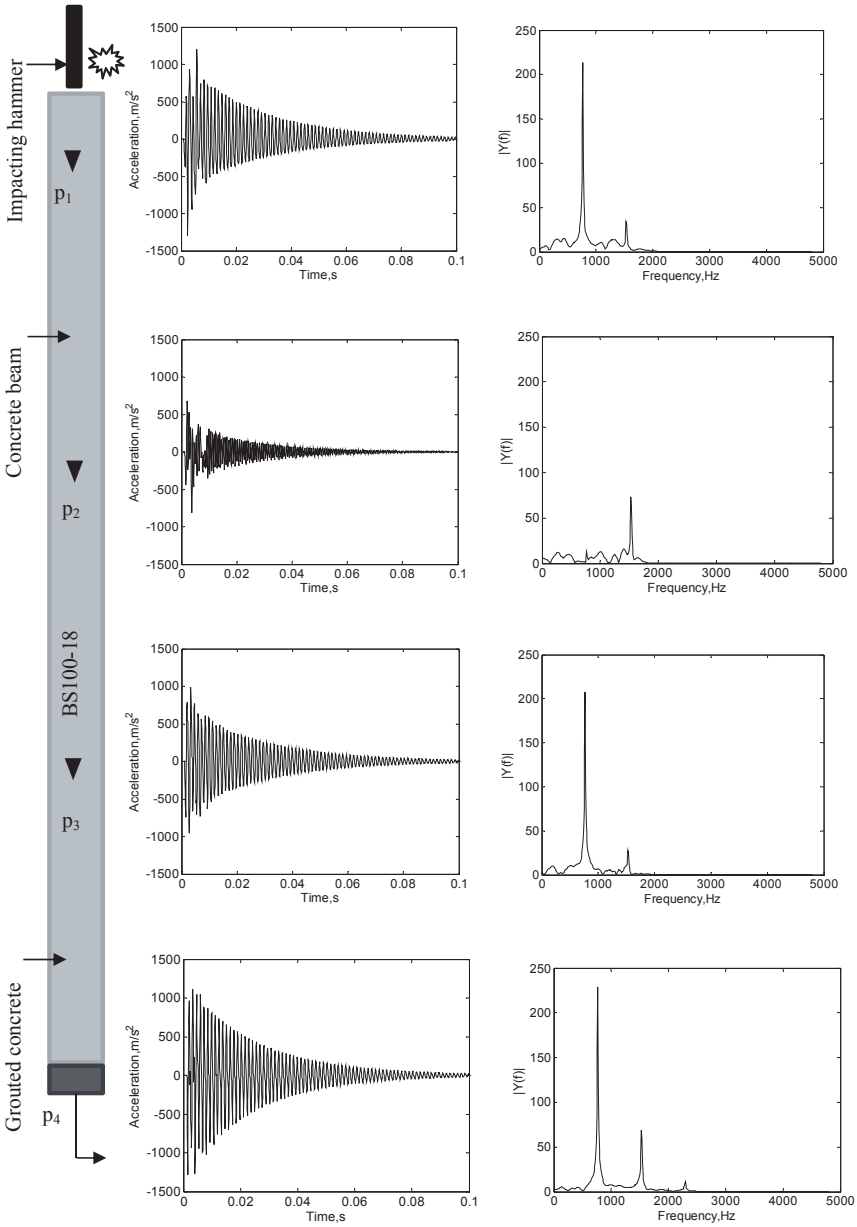

Figure 4.16: Calculated acceleration-time history and frequency spectra, for an impact velocity of 1.85 m/s.
Beräknad accelerations-tid och frekvensspektra för anslagshastigheten 1.85 m/s.

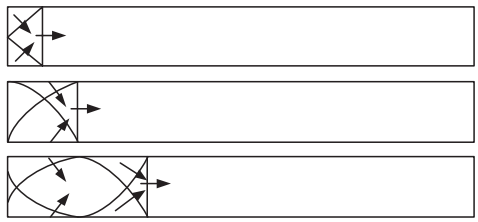

Figure 4.17: Release waves on the surface of the beam [28].
Avlastningsvågor på ytan av balken [28].

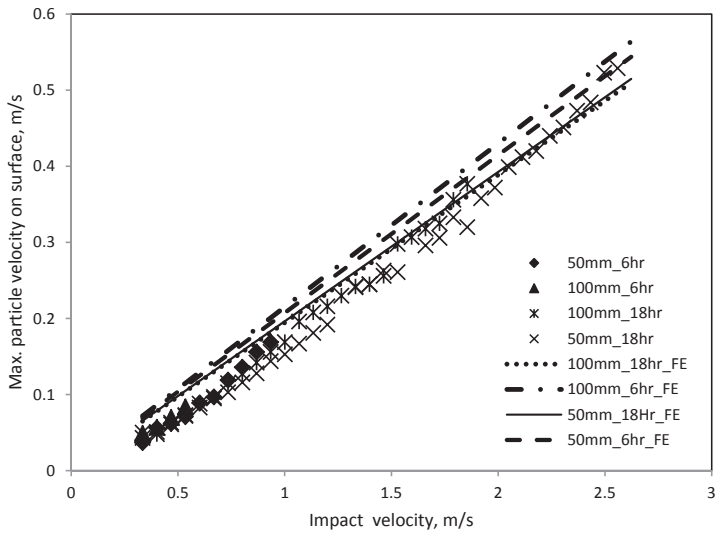

Figure 4.18: Measured maximum particle velocity on the surface of 50 and 100 mm shotcrete of 6 and 18 hours shotcrete age, compared to the corresponding FE results [7].
Uppmätt maximal partikelhastighet på ytan av 50 och 100 mm sprutbetong vid 6 och 18 timmars sprutbetongålder, jämfört med motsvarade FE resultat [7].

4.5 Shotcrete bond stresses

In order to show the dynamic stress in the shotcrete, an example from a FE analysis is presented in Figure 4.19. In this figure, the average stresses over the shotcrete elements

closest to the rock surface are shown as function of time. A summary of the average stresses from the FE analyses are plotted in Figure 4.20. The lines show the relations between impact velocity and maximum stresses in the shotcrete, at the shotcrete-rock interface.

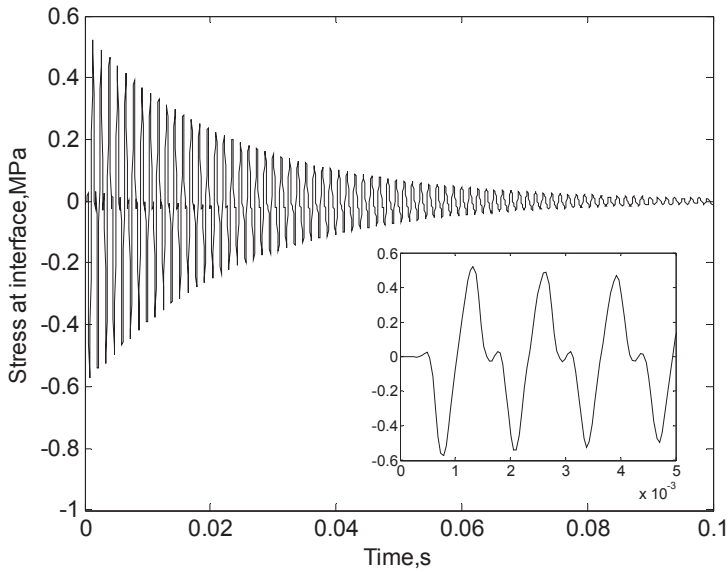

Figure 4.19: Simulated stress in the shotcrete element closest to the test-beam for 100 mm shotcrete, 18 hours old with the impact velocity 1.85 m/s.
Simulerade spänningar i sprutbetongelementet närmast balken för 100 mm sprutbetong, 18 timmar gammal och med anslagshastigheten 1.85 m/s.

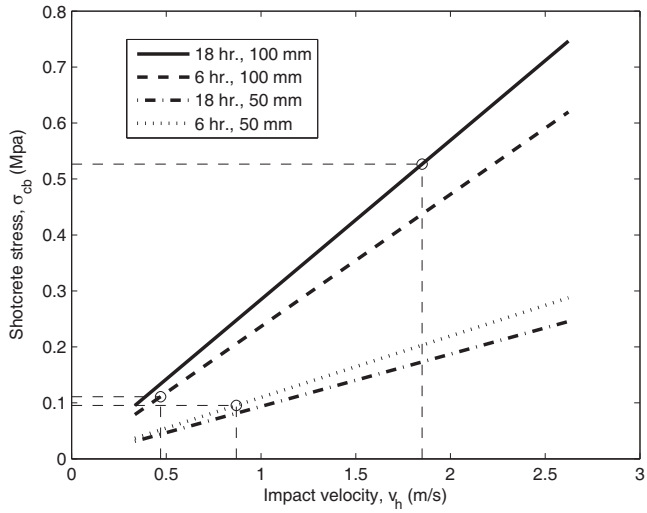

Figure 4.20: Maximum stress in the shotcrete element closest to the test-beam. From FE analyses for 50 and 100 mm shotcrete, 6 and 18 hours old [7].
Maximala spänningar i sprutbetongelementet närmast balken. Från FE analyser för 50 och 100 mm sprutbetong, 6 och 18 timmar gammal [7].

5. Conclusions

5.1 Discussion

A strip of rock could, in this laboratory investigation, with good accuracy be represented by a suspended concrete beam. Also, aging cement mortar showed similar properties as observed for shotcrete in tunnel environments. When such a concrete beam with mortar was used in the laboratory model an impacting hammer could initiate the same type of stress waves as from blasting in good quality rock. The assumptions that previously have been used in numerical calculations with an elastic stress-wave model [6] are thus realistic. This was here also verified through comparison with the results from a FE model able to describe the rock-shotcrete system loaded in the longitudinal direction.

The concrete beam used in the laboratory investigation had a wave propagation velocity close to 4000 m/s and can thus in this respect be accepted as a substitute for a beam of rock corresponding to good quality granite. In addition, the density of the concrete was close to that of granite with a corresponding modulus of elasticity of approximately 37 GPa, also accurate in this respect. The laboratory and numerical results given in Figures 4.13 and 4.17 show a good correspondence between measured and calculated shotcrete response, in both time and frequency domains. From the figures, it can be seen that the longitudinal vibrations are dominated by the first vibration mode and that there is very little contribution from the second mode. The frequencies of the first and the second mode are around 800 and 1600 Hz. Very small contributions from the third and higher modes can be seen. The used sampling frequency of 9600 Hz is therefore sufficient in this case.

The growth in bond strength of the mortar, used as a substitute for shotcrete, is initially faster than that of the compressive strength, when related to the levels reached during a relatively short time span of 24 hours. It should be noted that the tests were performed in laboratory environment under room temperature (approx. +20º C) which naturally is higher than in e.g. a normal tunnel environment, where also contact with the relatively colder rock affects the hardening of cementitious materials. The strength levels reached are however still comparable with previous observations, which are summarized in

section 1.3, and the mortar can therefore be accepted as an accurate substitute for shotcrete in these tests.

The relation between impact velocities and particle velocities measured on the shotcrete surface is shown in Figure 4.18, together with the corresponding results from the FE model. Note that the straight lines representing the FE results diverge as the impact velocity increases, depending on age and thickness of the shotcrete. The highest surface vibration velocity for each case in Figure 4.18 agrees with previously observed maximum particle velocities (see section 1.2). For young (1–25 hours old), approximately 50 mm thick shotcrete the highest velocity measured for an undamaged lining is within 0.5–1.0 m/s [9]. The results marked in Figure 4.18 show that for 50 mm shotcrete values of around 0.2 m/s were measured at 6 hours of age and > 0.55 m/s at 18 hours. Numerical modelling has previously been used to show that these limits should be within 0.15–0.30 m/s [8]. For 100 mm thick shotcrete the corresponding limits are lower, approximately 0.10 and 0.40 m/s, respectively, which also are in good correspondence with the numerical results that gives a value just under 0.30 m/s for the thicker shotcrete. The results in Figure 4.20 show that the limit values for 6 hours old shotcrete correspond to a bond stress (σ_{cb}) of about 0.1 MPa. For 100 mm thickness, it is about 0.55 MPa at 18 hours. These results are in good agreement with the bond strength 0.1 and 0.7 MPa, respectively, given in section 1.3. If the line representing 18 hours old, 50 mm thick shotcrete is extrapolated, $\sigma_{cb} \approx 0.55$–0.70 MPa and a relatively high impact velocity of about 5.5–7.5 m/s will be reached.

The effect of the aging shotcrete is studied in [7]. When the two materials rock and shotcrete have identical properties, the stress waves will pass through as if these were one material. For very young shotcrete with a low propagation velocity, the impedance ratio is low and therefore a relatively large fraction of the wave energy is reflected back into the rock. Young shotcrete will thus be exposed to lower stress levels compared to stiffer shotcrete from the same incoming wave.

5.2 General conclusions

An important goal of the entire project is to obtain knowledge on how close in time and distance, to shotcrete blasting can take place. The tests described in this report give data to be used in the verification of numerical models and to provide background for future recommendations for practical use in civil engineering underground work, tunnelling and mining. A type of finite element models suitable for dynamic analysis of shotcrete exposed to vibrations from blasting has been developed [5], implemented using the Abaqus/Explicit program [1]. The models based on 2D solid finite elements makes it

possible to perform more accurate analyses than with the previously used prototype models, giving detailed results. In addition, three existing prototype (engineering) models [6] have been compared and evaluated with respect to the results from the finite element models. The stress wave and structural dynamic properties have been compared with focus on the relation between applied loads and calculated displacements and stresses. The analysis results have also been compared to results previously obtained in-situ (see section 1.3) and those from this laboratory study.

An important goal was to identify factors and material properties that greatly affect the analysis results and how these should be accounted for in the numerical models. It was seen that it is important to include rock damping in the models to include the effect of decreasing stress levels as the disturbing waves propagate through the rock, away from the source of blasting. It was also observed that the modulus of elasticity for the rock is important since it affects the wave propagation velocity and the frequency content of the stresses that reach the shotcrete-rock interface. The complex superposition of incident, reflected and transmitted stress waves at the interface can be illustrated by the results from the suggested analytical models [5].

The results show how the explosion generate stress waves that propagates towards the free, shotcreted tunnel surface. Due to this motion, the stresses on the shotcrete vary in time, the stresses being the sum of the incident and reflected stress waves. It is demonstrated that the peak stress occur later for longer distances while the stress levels decrease. The wave arrives at the point of observation as compressive stress, directly followed by the tensile maximum which is critical with respect to bond failure at the interface.

An example of the minimum ages at the time of blasting for 100 mm thick shotcrete are compiled and presented in Figure 5.1. The results are calculated for detonations of 0.5, 1.0 and 2.0 kg of explosive at 2.2, 3.0 and 5.0 m from shotcrete on a rock surface [5].

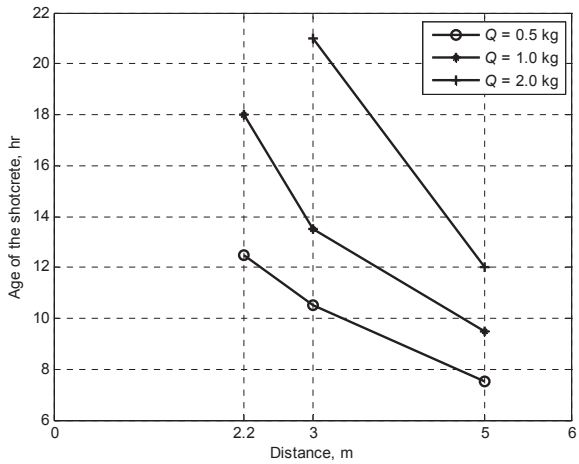

Figure 5.1: Compiled minimum age for 100 mm thick shotcrete vs the distance from detonation [5].
Minimiålder för 100 mm sprutbetong som funktion av avståndet från detonationen [5].

It was demonstrated [5] how the analysis method can be used to identify acceptable limits to be included in practical recommendations. An example of recommended minimum safe distances and minimum ages are given in Tables 5.1 and 5.2, adding further information to existing, preliminary recommendations [8]. The recommendations for minimum safe distances to a point of detonation of Q = 2 kg of explosives are given in Table 5.1. The results from [11] are also given for comparison. The table thus give a comparison between values for varying rock quality and load frequencies. Note that the safe distances for E_{rock} = 16 GPa and f = 1265 Hz are lower than for E_{rock} = 40 GPa and f = 2000 Hz, which is reasonable due to the different excitation values as well as to the lower values for the modulus of elasticity that represent the occurrence of cracks and imperfections. Note that an increase in load frequency leads to higher load levels and longer safe distances. Furthermore, recommended minimum age for 100 mm thick shotcrete subjected to detonation of 0.5, 1.0 and 2.0 kg of explosive at 2.2, 3.0 and 5.0 m from shotcrete are given in Table 5.2. For comparison the table also contain the corresponding values obtained for the slower developing bond strength curve from [8].

With detailed information about tunnel geometry, rock types, etc., the suggested method will make it possible to establish a complete set of guidelines for efficient use of shotcrete in environments exposed to vibrations. By implementing these in the

construction planning it will be possible to reduce the production time for underground construction and tunnelling, also with a high degree of safety for the workers.

Thus, the suggested modelling approach is a suitable tool for the work of determining guidelines for practical use in tunnelling and underground work in hard rock involving blasting close to shotcrete.

Table 5.1: Recommended minimum safe distance from the detonation of Q = 2 kg. *Rekommenderad minsta säkert avstånd från detonationen av Q = 2 kg.*

Rock and load characteristics	Shotcrete thickness		
	100 mm	50 mm	25 mm
E_{rock}= 16 GPa and f = 1265 Hz	1.8 m	1.0 m	0.7 m
E_{rock}= 40 GPa and f = 2000 Hz	2.5 m	1.5 m	0.8 m
E_{rock}= 40 GPa and f = 2500 Hz [11]	3.5 m	1.9 m	1.2 m

Table 5.2: Recommended minimum age for 100 mm thick shotcrete. The values within parentheses refer to the bond strength from [8]. *Rekommenderat minimiålder för 100 mm tjock sprutbetong. Resultat inom parantes refererar till vidhäftningshållfasthet från [8].*

Distance form explosive R	Detonation Q		
	0.5 kg	1.0 kg	2.0 kg
2.2 m	12 hrs. (>24 hrs.)	18 hrs. (>48 hrs.)	*
3.0 m	10 hrs. (24 hrs.)	13 hrs. (>24 hrs.)	21 hrs. (>48 hrs.)
5.0 m	7 hrs. (9 hrs.)	9 hrs. (21 hrs.)	12 hrs. (>24 hrs.)

*Not possible to obtain a sufficiently high bond strength.

5.3 Further research

The further work will continue with experimental investigations, also for shotcrete older than 24 hours. Material studies have been initiated [15] with the goal to describe the time dependence of shotcrete material properties such as compressive and tensile strengths, modulus of elasticity, shrinkage, creep and also bond strength related to various rock types. The following tests will also focus on the effect of cracked rock and variations in frequency content of the incoming stresses. This also needs to be compared to observations from tunnel environments. The finite element model will be developed

to facilitate analysis of rock-shotcrete sections with various geometries in two and three dimensions.

A further development of the presented type of finite element models [5] will be an important task for the future research. The goal is to establish well-defined limits for safe blasting, with respect to both shotcrete age and distance to the vibration source. The models will be used to study more complex geometries than before, such as construction of multiple tunnels, parallel tunnels, crossing tunnels and also stress waves with oblique impacts. The effect of different shotcrete material properties should be investigated, with focus on young and hardening shotcrete, but also accounting for possible inclusion of fibres. The effect of additional reinforcing elements, such as rock bolts, cables and wire mesh, can also be included.

Cases with multiple explosive charges will also be studied, aiming at finding the least damaging sequence of detonation using different delay times. The models can be further developed to also include the loading plan for the blasting rounds, i.e. initiation of explosives with a time interval. The initiation sequence of the explosives can e.g. be assumed according to the experiments performed at ASPE [30] and TASQ [32] tunnels in Sweden. In addition, the effect of loading density and rock mass properties along the charge hole will be investigated. The models can also be adjusted to include the effect of both intact rock and a zone of rock fractured due to blasting, situated around the tunnel perimeter. It will thus, by applying different modulus of elasticity to the two rock areas, be possible to study the protecting, filtering effect that the cracked rock volume has. Non-linear properties and behaviour of the rock and shotcrete can be introduced, making it possible to describe partial shotcrete failure.

Further in-situ measurements are required in order to establish a complete set of guidelines for efficient use of shotcrete in environments exposed to vibrations. Detailed information about tunnel geometry, rock types and plans for blasting operation must be used as input in the finite element analyses that will be used for evaluation of the measurement results. The material properties of shotcrete must also be investigated further, in laboratory tests that also include comparison with in-situ results and observations.

Bibliography

[1] ABAQUS User's Examples and Theory Manual, Version 6.10.

[2] Ahmed, L., Ansell, A., "A comparison of models for shotcrete in dynamically loaded rock tunnels". In: *Shotcrete: Elements of a system*. London: Taylor & Francis Group, 2010.

[3] Ahmed, L., Ansell, A., "Experimental and numerical investigation of stress wave propagation in shotcrete". In: *Nordic concrete research: Research projects,* 2011.

[4] Ahmed, L., Ansell A., "Finite element simulation of shotcrete exposed to underground explosions". *Nordic Concrete Research*, 45, 59–74, (2012).

[5] Ahmed, L., "*Models for analysis of shotcrete on rock exposed to blasting*". Licentiate thesis. Stockholm: KTH Concrete constructions; May 2012.

[6] Ahmed, L., Ansell, A., "Structural dynamic and stress wave models for analysis of shotcrete on rock exposed to blasting". *Engineering Structures*, 35, 11-17, (2012).

[7] Ahmed, L., Ansell, A., "Laboratory investigation of stress waves in young shotcrete on rock". *Magazine of Concrete Research*, 64, 899–908,(2012).

[8] Ansell, A., "Dynamic finite element analysis of young shotcrete in rock tunnels". *ACI Structural Journal,* 104, 84–92 (2007).

[9] Ansell, A., "*Dynamically Loaded Rock Reinforcement*". PhD thesis. Stockholm: KTH Structural Engineering; 1999.

[10] Ansell, A., "In situ testing of young shotcrete subjected to vibrations from blasting". *Tunnelling and Underground Space Technology*; 19, 587–596 (2004).

[11] Ansell, A., "Recommendations for shotcrete on rock subjected to blasting vibrations, based on finite element dynamic analysis". *Magazine of Concrete Research*, 57, 123–133 (2005).

[12] Barbo, T., Sprϕytebetong – betongteknologi. Heftfasthet (Sprayed concrete – concrete technology. Bond strength, in Norwegian), Kontor for fjellsprengningsteknikk, Oslo, 1964.

[13] Barrett, S., McCreath, D., "Shotcrete support design in blocky ground: Towards a deterministic approach". *Tunnelling and Underground Space Technology*, 10, 79–89 (1995).

[14] Benatar, A., Rittel, D., Yarin, A. L., "Theoretical and experimental analysis of longitudinal wave propagation in cylindrical viscoelastic rods". *Journal of the Mechanics and Physics of Solids*, 51, 1413–1431 (2003).

[15] Bryne, L. E., Holmgren, J., Ansell, A., "Experimental investigation of the bond strength between rock and hardening sprayed concrete". Proceedings of the *Sixth International Symposium on Sprayed Concrete*, Norwegian Concrete Society, Tromsø , 2011.

[16] Dowding, C. H., "*Construction Vibrations*". Upper Saddle River: Prentice-Hall 1996.

[17] Ellison, T., "*Vidhäftningsprovning Södra länken Stockholm*" (*Bond strength testing at Södra länken Stockholm*, in Swedish), Test report, Besab, Gothenburg, 2000.

[18] Hahn, T., Holmgren, J., "Adhesion of shotcrete to various types of rock surfaces and its influence on the strengthening function of shotcrete when applied on hard jointed rock". In: *Proceedings of the 4th International Congress on Rock Mechanics*. Montreux: International Society for Rock Mechanics, 1979.

[19] Holmgren, J., "*Bergförstärkning med sprutbetong* " (*Rock reinforcement with shotcrete, in Swedish*). Vattenfall, Vällingby, 1992.

[20] Karlsson, L., "*Sprutbetong mot olika bergytor*" (Shotcrete on various rock surfaces, in Swedish). Byggforskningsrådet, Stockholm, 1980.

[21] Kendorski, F. S., Jude, C. V., Duncan, W. M., "Effect of blasting on shotcrete drift linings". *Mining Engineering*; 25, 38–41 (1973).

[22] Kinsler, L. E., Frey, A. R., Coppens, A. B., Sanders, J. V., "*Fundamentals of acoustics*". 4th ed. Wiley, New York, 1993.

[23] Kumar, D., Behera, P.K., Singh, U.K., "Shotcreting and its adhesion strength". *Electronic Journal of Geotechnical Engineering*, 7, (2002).

[24] Malmberg, B., "*Sprutbetong – uppföljning av sprutbetongprovningar på Grödingebanan*", (*Shotcrete – evaluation of shotcrete testing at Grödingebanan*, in Swedish), No. T93-913/34, Borlänge, 1993.

[25] Malmgren, L., and Nordlund, E., "Interaction of shotcrete with rock and rock bolts – A numerical study". *International Journal of Rock Mechanics and Mining Sciences*, 45, 538–553 (2008).

[26] Mathworks *Matlab*. See http://www.mathworks.com/products/matlab/ for further details. Accessed 07/07/2011, (2011).

[27] McCreath, D. R., Tannant, D. D., Langille, C. C., "Survivability of shotcrete near blasts". In: *Rock Mechanics*. Rotterdam, Balkema, 1994.

[28] Meyers, M. A., "*Dynamic behavior of materials*". New York: John Wiley & Sons; 1994.

[29] Nakano, N., Okada, S., Furukawa, K., Nakagawa, K., "Vibration and cracking of tunnel lining due to adjacent blasting", (in Japanese, Abstract in English). *Proceedings of the Japan Society of Civil Engineers*, 3, 53–62 (1993).

[30] Nyberg, U, Harefjord, L., Bergman, B., Christiansson, R., "*Monitoring of vibrations during blasting of the APSE* ". SKB report R-05-27, Sweden, 2008.

[31] O'Donnell, J. D. P. Sr., Tannant, D. D., "Pull tests to measure the in situ capacity of shotcrete", In: *CIM-AGM*, Montreal, 1997.

[32] Olsson, M., Niklasson, B., Wilson, L., Andersson, C., "*Experiences of blasting of the TASQ tunnel*". SKB report R-04-73, Sweden, 2004.

[33] Saiang, D., Malmgren, L., Nordlund, E., "Laboratory tests on shotcrete-rock joints in direct shear, tension and compression". *Rock Mechanics and Rock Engineering* 38, 275–297 (2005).

[34] Silfwerbrand, J., "*The influence of traffic-induced vibrations on the bond between old and new concrete*", Bulletin 1992 No.158. Dept. of Structural Mechanics and Engineering, KTH, Stockholm, 1992.

[35] SS 13 72 43 Concrete testing–hardened concrete – adhesion strength, 1987. Swedish standard, in Swedish.

[36] *The Fundamentals of Signal Analysis*, Application Note 243, Hewlett-Packard, 1985.

[37] Thomson, W. T., "*Theory of Vibration with Applications*". 4th ed. Prentice hall, Englewood Cliffs, 1993.

[38] Vandewalle, M., "*Dramix – Tunnelling the World*". *With 7 Reference Projects*, 6th edn. N.V. Bekaert S.A., Zwevegem, 1998.

[39] Wood, D. F., Tannant, D. D., "Blast damage to steel fibre reinforced shotcrete". In: *Fibre-reinforced Concrete–Modern Developments*. Vancouver: University of British Columbia Press, 1994.

BeFo

Box 5501
SE-114 85 Stockholm

info@befoonline.org • www.befoonline.org
Visiting address: Storgatan 19

ISSN 1104-1773